International Global Navigation Satellite Systems Association
IGNSS Conference 2016

Colombo Theatres, Kensington Campus, UNSW Australia
6 – 8 December 2016

Ambiguity Resolution (PPP-AR) For Precise Point Positioning Based on Combined GPS Observations

Shuyang Cheng and Jinling Wang

School of Civil and Environmental Engineering, University of New South Wales, Sydney, NSW 2052, Australia

Phone: +61 416 866 545 Fax: +61 2 9385 6139 Email: *shuyang.cheng@student.unsw.edu.au*

ABSTRACT

Precise point positioning (PPP) which uses ionosphere-free combination has been investigated for many years. In such conventional PPP model, the ambiguity parameters cannot be resolved to integers due to uncalibrated phase biases. These biases can be compensated by decoupled satellite clock (DSC), or fractional cycle bias (FCB), or integer recovery clock (IRC). These bias compensations are all based on ionosphere-free PPP (IF-PPP) and Melbourne-Wubbena combination in which the wide-lane (WL) ambiguity and narrow-lane (NL) ambiguity are fixed successively. Their performances with numerical analysis need to be further investigated. In addition, the vertical accuracy with PPP-AR is much worse than the horizontal component due to many factors, one of which is the limited accuracy of troposphere correction or weak zenith wet delay (ZWD) estimation.

In this study, the IRC and FCB based PPP-AR methods with ionosphere-free PPP are systematically compared. Firstly, we introduce the integer property recovery of these methods to justify their equivalence. Moreover, numerical analysis is conducted to evaluate the performances of these methods. The results indicate that although these methods are equivalent in theory, the performance is slightly different due to the biased property of FCB estimation and different processing strategies in IRC based PPP-AR. Furthermore, it is demonstrated that vertical positioning accuracy can be improved with proper troposphere constraints.

KEYWORDS: Precise Point Positioning, Integer Ambiguity Resolution, Fractional Cycle Bias, Integer Recovery Clock, Troposphere Delay Constraint

1. INTRODUCTION

Precise Point Positioning (PPP) is a Global Navigation Satellite System (GNSS) positioning method to precisely determine the position of any point around the globe by using a single GNSS receiver with precise orbit and clock products, such as from International GNSS Service (IGS). It was firstly proposed in the 1990s to achieve positioning accuracy at decimetre even to centimetre level (Zumberge *et al.*, 1997; Kouba and Héroux, 2001). Currently it has become a useful positioning tool in a number of potential applications, such as aerial triangulation (Shi et al. 2016), GPS meteorology (Li et al. 2015), earthquake/tsunami monitoring and early warning (Li et al. 2013a), etc.

In the traditional mathematical model of PPP, dual-frequency code and phase observations are combined to form ionosphere-free observations, which can eliminate the lower order term (about 99%) of ionospheric error (Kouba and Héroux, 2001). But the linearly combined observations also cause several adverse effects, e.g. amplification of observation noises and multipath effects. Externally derived ionospheric information cannot be incorporated in the ionosphere-free model. In addition, the ambiguity parameter is treated as real value in conventional PPP and it usually takes about 30min until the positioning accuracy of 10cm is obtained (Bisnath and Gao 2007), which prevents PPP from being widely used in real-time applications.

PPP-AR is expected to improve the desired positioning accuracy with short convergence time. Many researchers have contributed to the development of PPP-AR methods over the years. With various methods to compensate phase biases, three typical methods are well-known: fractional cycle bias (FCB) method (Ge et al. 2008), integer recovery clock (IRC) method (Laurichesse et al. 2008) and decoupled satellite clock (DSC) method (Collins 2008). Teunissen and Khodabandeh (2015) justified that they are theoretically equivalent. Similar conclusions can be found in the publications of, for instance, Geng et al. (2010), Shi and Gao (2014), etc. A significant improvement of positioning accuracy can be achieved by PPP-AR as compared with ambiguity-float PPP, especially in the east component (Ge et al. 2008). But the time to first fix (TTFF) is still relatively long, about 20 min. However, the vertical accuracy with PPP-AR is still much worse than the horizontal component due to many factors, one of which is the limited accuracy of troposphere correction or weak ZWD estimation.

In order to overcome the drawback of traditional PPP, uncombined PPP (U-PPP) model was proposed (Keshin *et al.*, 2006). In this model, line of sight (LOS) ionosphere delay on L1 frequency is estimated as an unknown parameter for each satellite and epoch. Li et al. (2013b) modified the FCB method and extended it to U-PPP model. In this implementation, the slant ionosphere delays are estimated with proper temporal and spatial constraints while the FCBs on L1 and L2 frequency can be estimated separately. The TTFF can be shortened to several minutes by employing such method.

Although many researchers have implemented different PPP-AR methods based on IF-PPP, few papers compare them systematically with numerical analysis. In this study, we compare the performances of FCB and IRC based PPP-AR methods. The impact of troposphere delay on PPP-AR is also analysed. The structure of the paper is as follows: In Section 2, the basic observation equations and the format of estimated FCB with IGS satellite clock and integer phase clock are presented in order to prove the equivalence of FCB and IRC based PPP-AR methods in terms of integer property recovery. In Section 3, the PPP-AR processing strategies

and troposphere delay modelling method to enhance PPP-AR performance are introduced. In Section 4, specific numerical analysis is conducted to validate the equivalence of FCB and IRC based PPP-AR methods. Meanwhile, the impact of troposphere delay on PPP-AR is also demonstrated. Finally, some concluding remarks are put forward and the future research issues are proposed.

2. FCB ESTIMATION WITH IGS SATELLITE CLOCK AND CNES INTEGER PHASE CLOCK

For a specific satellite *s* and receiver *r* pair, the observation equations of raw GPS pseudorange *P* and carrier phase *L* are expressed as:

$$P_{r,i}^{s} = \rho_{r}^{s} + cdt_{r} - cdt^{s} + T_{r}^{s} + I_{r,i}^{s} + D_{r,i} - D_{i}^{s} + \varepsilon_{p,i} \tag{1}$$

$$L_{r,i}^{s} = \rho_{r}^{s} + cdt_{r} - cdt^{s} + T_{r}^{s} - I_{r,i}^{s} + \lambda_{i}(N_{i}^{s} + \varphi_{r,i} - \varphi_{i}^{s}) + \varepsilon_{L,i} \tag{2}$$

where subscript i represents the frequency of GPS observation; ρ_{r}^{s} denotes the geometric distance; c is the speed of light in vacuum; dt_{r} and dt^{s} are receiver and satellite clock offset; T_{r}^{s} is the slant troposphere delay; $I_{r,i}^{s}$ is the slant ionosphere delay on frequency i; λ_{i} is the wavelength of the frequency i; N_{i}^{s} is the integer ambiguity on frequency i; $D_{r,i}$ and D_{i}^{s} are the receiver and satellite code instrumental delays on frequency i due to the transmitting and receiving hardware; $\varphi_{r,i}$ is the combination of receiver phase instrumental delay and initial phase bias on frequency i; φ_{i}^{s} is the combination of satellite phase instrumental delay and initial phase bias on frequency i; $\varepsilon_{p,i}$ and $\varepsilon_{L,i}$ are the measurement noises and multipath effects of pseudorange and carrier phase. Other error terms, such as relativistic effects, antenna phase centre offsets and variations (Schmid et al. 2005) of satellite and receiver, phase wind-up (Wu et al. 1993), tide loading and so on, are precisely corrected with corresponding models in advance. In order to fix integer ambiguities in (1) and (2), the phase biases need to be compensated.

2.1 FCB estimation with IGS satellite clock products

The satellite clock products from IGS can be expressed as (Dach et al. 2009):

$$cdt_{IGS}^{s} = cdt^{s} + D_{IF}^{s} \tag{3}$$

where $D_{IF}^{s} = (f_1^2 D_1^s - f_2^2 D_2^s)/(f_1^2 - f_2^2)$

The observation equations of ionosphere-free GPS pseudorange P_{IF} and carrier phase L_{IF} are expressed as:

$$\begin{aligned} P_{r,IF}^{s} &= \rho_{r}^{s} + (cdt_{r} + D_{r,IF}) - (cdt^{s} + D_{IF}^{s}) + T_{r}^{s} + \varepsilon_{p,IF} \\ &= \rho_{r}^{s} + c\widetilde{dt}_{r,IF} - cdt_{IGS}^{s} + T_{r}^{s} + \varepsilon_{p,IF} \end{aligned} \tag{4}$$

$$\begin{aligned} L_{r,IF}^{s} &= \rho_{r}^{s} + c\widetilde{dt}_{r,IF} - cdt_{IGS}^{s} + T_{r}^{s} + [B_{IF}^{s} + (\varphi_{r,IF} - \varphi_{IF}^{s}) - (D_{r,IF} - D_{IF}^{s})] + \varepsilon_{L,IF} \\ &= \rho_{r}^{s} + c\widetilde{dt}_{r,IF} - cdt_{IGS}^{s} + T_{r}^{s} + \tilde{B}_{IF}^{s} + \varepsilon_{L,IF} \end{aligned} \tag{5}$$

where $\widetilde{dt}_{r,IF}$ is the estimated receiver clock offset which absorbs the ionosphere-free code instrumental delays, and with:

$$D_{r,IF} = (f_1^2 D_{r,1} - f_2^2 D_{r,2}) / (f_1^2 - f_2^2) \tag{6}$$

$$B_{IF}^s = (f_1^2 \lambda_1 N_1^s - f_2^2 \lambda_2 N_2^s)/(f_1^2 - f_2^2) \tag{7}$$

$$\varphi_{r,IF} = (f_1^2 \lambda_1 \varphi_{r,1} - f_2^2 \lambda_2 \varphi_{r,2}) / (f_1^2 - f_2^2) \tag{8}$$

$$\varphi_{IF}^s = (f_1^2 \lambda_1 \varphi_1^s - f_2^2 \lambda_2 \varphi_2^s)/(f_1^2 - f_2^2) \tag{9}$$

In PPP-AR, $\tilde{B}_{IF}^s$ is often decomposed into integer WL ambiguity N_{WL}^s and float NL ambiguity $\tilde{N}_{NL}^s$ for ambiguity-fixing, *i.e.*:

$$\tilde{B}_{IF}^s = cf_2 N_{WL}^s/(f_1^2 - f_2^2) + \lambda_{NL}\tilde{N}_{NL}^s = cf_2(N_1^s - N_2^s)/(f_1^2 - f_2^2) + \lambda_{NL}\tilde{N}_{NL}^s \tag{10}$$

where λ_{NL} is the wavelength of NL combination, $\lambda_{NL} = c/(f_1 + f_2)$.

Float WL ambiguity can be calculated by taking the time average of the Melbourne-Wübbena (MW) combination observations (Melbourne 1985; Wubbena 1985):

$$\tilde{N}_{WL}^s = [(f_1 L_{r,1}^s - f_2 L_{r,2}^s)/(f_1 - f_2) - (f_1 P_{r,1}^s + f_2 P_{r,2}^s)/(f_1 + f_2)]/\lambda_{WL} \tag{11}$$

where λ_{WL} is the wavelength of WL combination, $\lambda_{WL} = c/(f_1 - f_2)$.

Firstly, $\tilde{N}_{WL}^s$ can be fixed to integer WL ambiguity N_{WL}^s based on the following equation:

$$\tilde{N}_{WL}^s = N_{WL}^s + FCB_{r,WL} - FCB_{WL}^s = N_1^s - N_2^s + FCB_{r,WL} - FCB_{WL}^s \tag{12}$$

By substituting (1), (2) and (11) into (12):

$$\begin{aligned} FCB_{r,WL} - FCB_{WL}^s = {} & \varphi_{r,1} - \varphi_{r,2} - (\varphi_1^s - \varphi_2^s) \\ & -[(f_1 D_{r,1} + f_2 D_{r,2} - f_1 D_1^s - f_2 D_2^s)/(f_1 + f_2)]/\lambda_{WL} \end{aligned} \tag{13}$$

After WL ambiguity is successfully fixed to correct integer $(N_1^s - N_2^s)$, by substituting (5) and (7) into (10), the derived float NL ambiguity can be expressed as:

$$\tilde{N}_{NL}^s = N_1^s + [(\varphi_{r,IF} - \varphi_{IF}^s) - (D_{r,IF} - D_{IF}^s)]/\lambda_{NL} \tag{14}$$

and:

$$\tilde{N}_{NL}^s = N_{NL}^s + FCB_{r,NL} - FCB_{NL}^s = N_1^s + FCB_{r,NL} - FCB_{NL}^s \tag{15}$$

By substituting (14) into (15):

$$FCB_{r,NL} - FCB_{NL}^s = [(\varphi_{r,IF} - \varphi_{IF}^s) - (D_{r,IF} - D_{IF}^s)]/\lambda_{NL} \tag{16}$$

By applying the single difference between satellites *j* and *k* to (13) and (16), the single-

differenced (SD) WL and NL satellite FCBs can be expressed as:

$$\nabla FCB_{WL}^{j,k} = \nabla\varphi_1^{j,k} - \nabla\varphi_2^{j,k} - [(f_1 \nabla D_1^{j,k} + f_2 \nabla D_2^{j,k})/(f_1 + f_2)]/\lambda_{WL} \quad (17)$$
$$\nabla FCB_{NL}^{j,k} = [f_1(\nabla\varphi_1^{j,k} - \nabla D_1^{j,k}/\lambda_1) - f_2(\nabla\varphi_2^{j,k} - \nabla D_2^{j,k}/\lambda_2)]/(f_1 - f_2) \quad (18)$$

where ∇ is the single differencing operator.

2.2 FCB estimation with CNES integer phase clock products

The integer phase clock products from Centre National d'Etudes Spatiales (CNES) used in IRC based PPP-AR can be expressed as (Loyer et al. 2012):

$$cdt_{CNES}^s = cdt^s + (f_1^2\lambda_1\varphi_1^s - f_2^2\lambda_2\varphi_2^s)/(f_1^2 - f_2^2) = cdt^s + \varphi_{IF}^s \quad (19)$$

IGS code clock is applied to code observations while CNES phase clock is applied to phase observations. Thus the ionosphere-free code observation equation is the same as (4). Assuming the estimated receiver clock offset in the phase observation equation is $dt_r{}'$:

$$\begin{aligned} L_{r,IF}^s &= \rho_r^s + cdt_r - (cdt^s + \varphi_{IF}^s) + T_r^s + B_{IF}^s + \varphi_{r,IF} + \varepsilon_{L,IF} \\ &= \rho_r^s + cdt_r{}' - cdt_{CNES}^s + T_r^s + \tilde{B}_{IF}^s{}' + \varepsilon_{L,IF} \end{aligned} \quad (20)$$

MW combination observations are still used in WL ambiguity fixing, thus the SD WL FCB is the same as (17). By substituting (7) and (20) into (10), the float NL ambiguity becomes:

$$\tilde{N}_{NL}^s{}' = N_1^s + (cdt_r + \varphi_{r,IF} - cdt_r{}')/\lambda_{NL} = N_1^s + FCB_{r,NL}{}' - FCB_{NL}^s{}' \quad (21)$$

$$FCB_{r,NL}{}' - FCB_{NL}^s{}' = (cdt_r + \varphi_{r,IF} - cdt_r{}')/\lambda_{NL} \quad (22)$$

By applying the single difference between satellites *j* and *k* to (22):

$$\nabla FCB_{NL}^{j,k}{}' = 0 \quad (23)$$

From the equations above, it can be concluded that the WL ambiguity fixing is the same for FCB and IRC based PPP-AR because MW combination observations are used. After correcting the SD NL FCB, the integer property of SD NL ambiguity can be recovered in FCB based PPP-AR. If integer phase clock is employed, the integer property of SD NL ambiguity can directly be recovered without any corrections according to (23). The only difference is that additional (phase) receiver clock offset needs to be estimated in the phase observation equation and the NL ambiguity of one satellite is fixed to arbitrary integer to define the ambiguity datum (Shi and Gao 2014) in IRC based PPP-AR. But the model redundancy still remains the same as FCB based PPP-AR. Thus these two methods are theoretically equivalent in terms of integer property recovery. Moreover, the fixed integer SD ambiguities are in fact double-differenced ambiguities according to Teunissen and Khodabandeh (2015).

3. PPP-AR AND TROPOSPHERE DELAY DERIVATION

3.1 PPP-AR processing strategy

The undifferenced satellite FCB can be generated from a global reference network by using the similar strategy discussed in Li et al. (2013b), quality control for least-squares estimation is also employed to reject potential outliers. In fact, we can only obtain the optimal estimate instead of the truth value of FCBs. After the undifferenced float ambiguities are obtained from float PPP solution, they are firstly transformed into SD format by choosing a reference satellite with highest elevation angle. Then PPP-AR can be conducted in two sequential steps. Firstly, after correcting SD WL satellite FCBs, the SD smoothed WL ambiguities can be easily fixed by rounding. After SD WL ambiguities are successfully fixed, SD NL ambiguities can be derived according to Eqs. (10) and corrected with SD NL satellite FCBs (not corrected in IRC based PPP-AR). Then Least-squares AMBiguity Decorrelation Adjustment (LAMBDA) method (Teunissen 1995) is applied to search for the optimal integer solution of SD NL ambiguities. Finally, the fixed SD WL and NL ambiguities are transformed back to IF ambiguities. In addition, the R/W-ratio and bootstrapped success rate test are used to validate the integer ambiguity solution. The test thresholds are set as 3.0 and 0.999, respectively.

It is crucial for the ambiguities to be correctly fixed. However, in many situations reliable ambiguity resolution is not feasible due to biases in the data, thus model strength is not enough to resolve the full set of ambiguities with a sufficiently high success rate. In those cases, Partial Ambiguity Resolution (PAR) can be useful. In order to resolve as many correct integer ambiguities as possible, a subset of the ambiguities is selected which can be fixed reliably. All the float ambiguities are sorted in the order of ascending estimate precision. Firstly, choose the first two ambiguities as the ambiguity subset, then try to fix this subset by LAMBDA and validate the integer solution. If all the validation tests pass, add the third ambiguity into the ambiguity subset. These procedures are repeated until the largest ambiguity subset is determined.

3.2 Troposphere delay interpolation

After successful and reliable PPP-AR, the resolved integer ambiguities can be converted to accurate range measurements and accurate troposphere delay can be determined if the station coordinates are fixed. In order to enhance the ambiguity resolution at a user station, the ambiguity-fixed and coordinate-fixed troposphere delay can be firstly retrieved from surrounding reference networks and then interpolated just like Network Real Time Kinematic (NRTK). As for PPP, we have modified the Linear Combination Method (LCM) method as (Han 1997):

$$\begin{bmatrix} 1 & 1 & \cdots & 1 \\ \Delta X_{1u} & \Delta X_{2u} & \cdots & \Delta X_{n,u} \\ \Delta Y_{1u} & \Delta Y_{2u} & \cdots & \Delta Y_{n,u} \end{bmatrix} \begin{bmatrix} \alpha_1 \\ \alpha_2 \\ \vdots \\ \alpha_n \end{bmatrix} = \begin{bmatrix} 1 \\ 0 \\ 0 \end{bmatrix} \tag{24}$$

with:

$$\sum_{i=1}^{n} \alpha_i = 1, \quad \sum_{i=1}^{n} \alpha_i^2 = MIN, \quad \sum_{i=1}^{n} \alpha_i \, \Delta X_{iu} = 0, \quad \sum_{i=1}^{n} \alpha_i \, \Delta Y_{iu} = 0 \tag{25}$$

where ΔX_{iu} and ΔY_{iu} are the differences of the plane coordinate between the reference stations and user station.

By applying Lagrange multipliers approach to (24) and (25):

$$\begin{bmatrix} 2 & & & & 1 & \Delta X_{1u} & \Delta Y_{1u} \\ & 2 & & & 1 & \Delta X_{2u} & \Delta Y_{2u} \\ & & \ddots & & \vdots & \vdots & \vdots \\ & & & 2 & 1 & \Delta X_{n,u} & \Delta Y_{n,u} \\ 1 & 1 & \cdots & 1 & & & \\ \Delta X_{1u} & \Delta X_{2u} & \cdots & \Delta X_{n,u} & & & \\ \Delta Y_{1u} & \Delta Y_{2u} & \cdots & \Delta Y_{n,u} & & & \end{bmatrix} \begin{bmatrix} \alpha_1 \\ \alpha_2 \\ \vdots \\ \alpha_n \\ \beta_1 \\ \beta_2 \\ \beta_3 \end{bmatrix} = \begin{bmatrix} 0 \\ 0 \\ \vdots \\ 0 \\ 1 \\ 0 \\ 0 \end{bmatrix} \tag{26}$$

where β_1, β_2 and β_3 are three Lagrange multipliers.

The interpolated atmosphere corrections at a user station can be derived by the following equation:

$$atom_{user} = \sum_{i=1}^{n} \alpha_i \, atom_i \tag{27}$$

where $atom_i$ are the atmosphere corrections at reference stations, α_i can be calculated by Eq.(26).

The accuracy of interpolated atmosphere corrections can be assessed by the residuals of atmosphere delay:

$$v_{atom} = atom_{interpol} - atom_{est} \tag{28}$$

where v_{atom} is the atmosphere delay residual, $atom_{interpol}$ is the interpolated atmosphere delay, and $atom_{est}$ is the estimated atmosphere delay in PPP-AR.

At a user station, the atmosphere delay can be constrained by the interpolated atmosphere corrections with proper stochastic models which are determined by the interpolation accuracy.

4. NUMERICAL ANALYSIS

4.1 FCB Estimation results

In order to evaluate the performance of FCB estimation, around 160 globally distributed IGS stations on DOY 183, 2016 were selected. Both IGS satellite clock and CNES integer phase clock were used to derive FCBs. FCB of one satellite is fixed to zero. WL FCB could be estimated as a daily constant for each satellite due to its long-term stability, while NL FCB was estimated as a constant every 15 min thus there are 96 sets of NL FCBs in total in one day.

The quality of FCB estimation can be indicated by the posteriori residuals of float ambiguities used in FCB estimation. Figure 2 shows the residuals of WL ambiguities and NL ambiguities in the randomly selected 50th session. In general, a more consistent FCB estimation is expected if the residuals are close to zero. It can be seen that the Root Mean Square (RMS) of WL ambiguities is about 0.1 cycles while the RMS of NL ambiguities in the 50th session is about 0.07 cycles, which indicates a good consistency between the estimated FCBs and input float ambiguities.

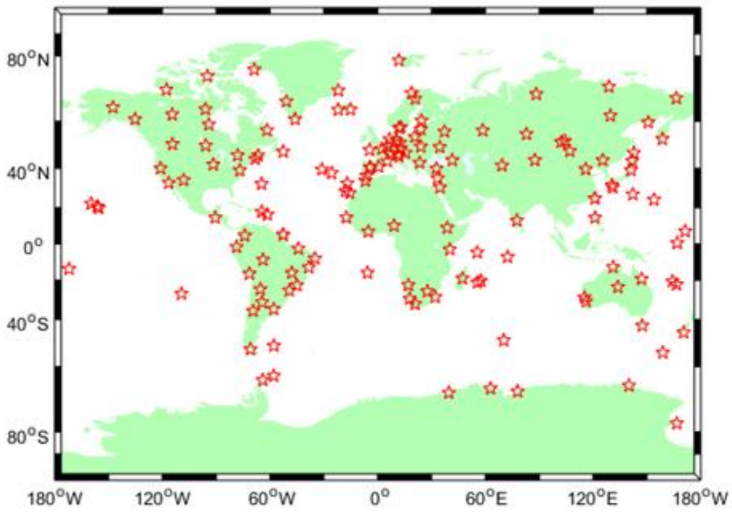

Figure 1. Distribution of selected IGS stations

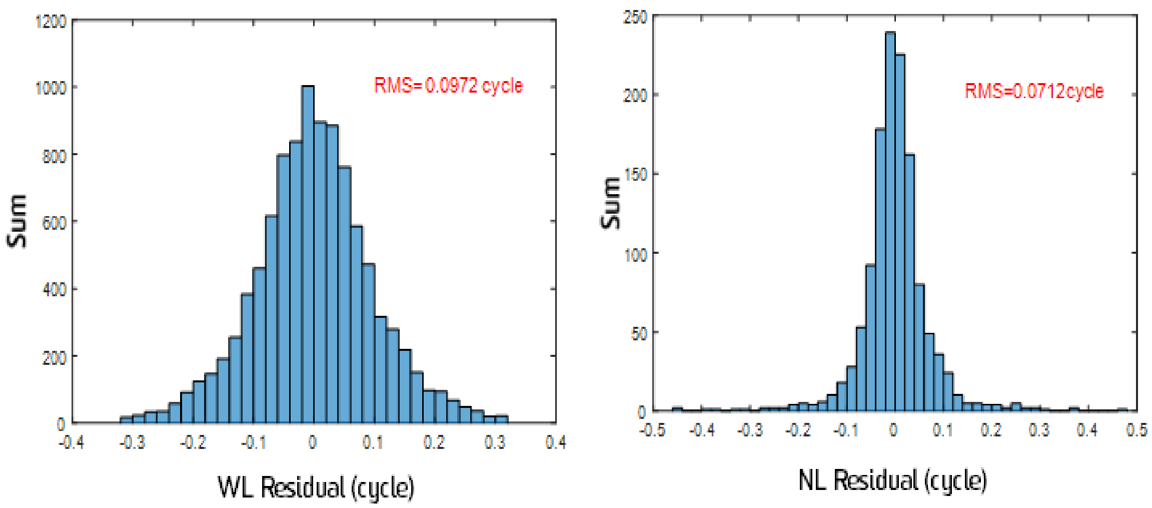

Figure 2. Residuals of WL ambiguities (*left*) and NL ambiguities in the 50th session (*right*)

If the integer phase clock is employed in FCB estimation, according to Section 2, the SD WL FCB should be the same as the estiamted FCB with IGS satellite clock while the SD NL FCB should be zero. Thus it can be used to analyze the biased property of FCB estimation. The difference between the estimated SD WL FCBs with IGS satellite clock and integer phase clock are plotted in Figure 3 while the 96sets of SD NL FCBs estimated with integer phase clock are plotted in Figure 4. The difference of SD WL FCB is below 0.04 cycles for all the satellites. SD NL FCBs are below 0.1 cycles for all the satellites and the RMS is about 0.01 cycles. Thus the bias of FCB estmation is relatively small and the estimated high-accuracy FCBs can be used for reliable PPP-AR.

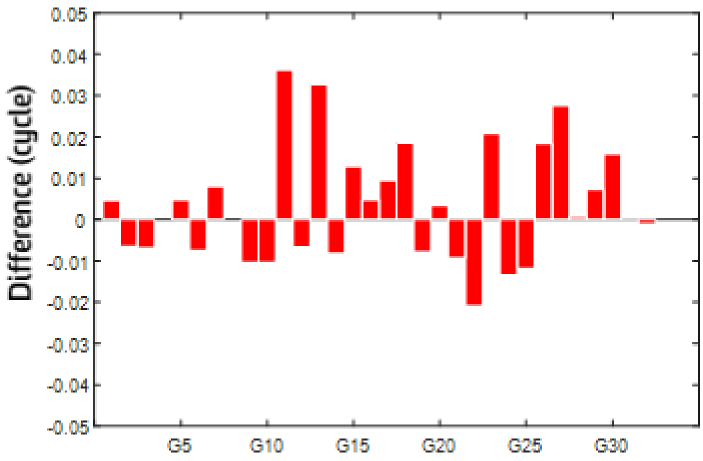

Figure 3. Difference between the estimated SD WL FCBs with IGS satellite clock and integer phase clock (G31 as the reference satellite)

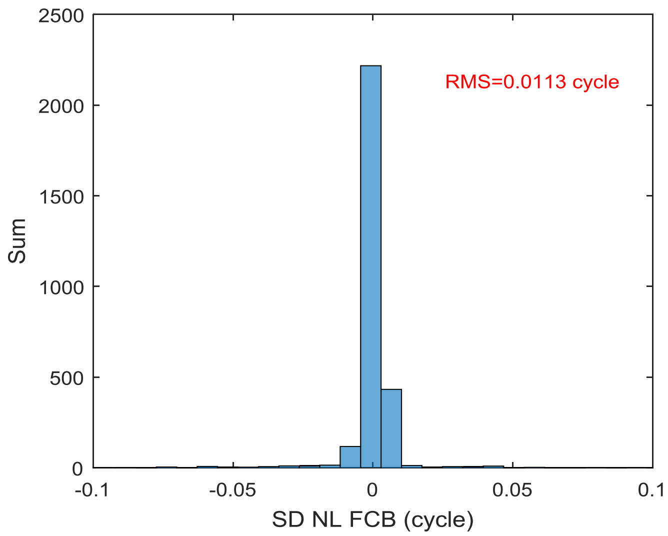

Figure 4. SD NL FCBs estimated by integer phase clock (G31 as the reference satellite)

4.2 Comparision of FCB and IRC based PPP-AR results

155 stations from CORSnet-NSW were used in PPP-AR and none of them were used in FCB estimation. For each station, the 24-hour data was divided into 24 hourly sessions. In total, there are 3720 sessions. All the datasets were processed in static mode with FCB and IRC based PPP-AR. The ambiguity-fixed solutions were compared with the true value of the station coordinate to obatin the position error. PPP-AR performance was evaluated in terms of positioning results, TTFF and correct fixing rate.

- Correct fixing rate

We regard the positioing results at and before the first ambiguity-fixed epoch as the PPP-fixed and PPP-float solution respectively. The ambiguity is assuemd to be wrongly fixed if the 3D positioning bias of PPP-fixed solution is larger than 5 cm and the horizontal positioning bias

of PPP-fixed solution is larger than PPP-float solution. Based on this assumption, the correct fixing rate of PPP-AR can be calculated, and are shown in Table 1.

PPP-AR methods	Total Solution	Correct Solution	Correct Fixing Rate
FCB	**3683**	**3652**	**99.16%**
IRC	**3684**	**3654**	**99.19%**

Table 1. Correct fixing rate of FCB and IRC based PPP-AR

It can be seen that the number of total solutions is below 3720 because ambiguity-fixed solution cannot be obtained in 1 hour for some sessions. The correct fixing rate of FCB and IRC based PPP-AR are nearly the same (above 99%) and the ambiguity search and validation approaches do not always perform well for PPP-AR in all cases.

- Static positioning results

After removing the wrong PPP-AR solutions, the RMS of positioning biases in east, north and up directins for the remaining sessions are summarized in Table 2.

PPP-AR methods	East	North	Up	3D
FCB (float)	**7.71**	**2.80**	**8.04**	**11.49**
FCB (fixed)	**0.88**	**0.60**	**3.67**	**3.82**
IRC (float)	**8.08**	**2.90**	**8.03**	**11.75**
IRC (fixed)	**0.75**	**0.55**	**3.00**	**3.16**

Table 2. RMS of positioning bias for FCB and IRC based PPP-AR (Unit: cm)

It can be seen that the positioning results of IRC based PPP-AR is slightly better than FCB based PPP-AR, because the NL FCBs are fully absorbed in the integer phase clock thus FCB estimation which is actually a biased solution can be avoided in IRC based PPP-AR. In addition, ambiguity fixing provides a considerable improvement in the positioning accuracy, especially in the east component (from about 8 cm to below 1cm), but the vertical accuracy (about 3~4 cm) is still worse than the horizontal accuracy (below 1cm), which may be due to the unmodelled errors in troposphere delay. The impact of troposphere delay on PPP-AR will be analysed in the next section.

- TTFF

The distribution of TTFF for FCB and IRC based PPP-AR is demonstrated in Figure 5.

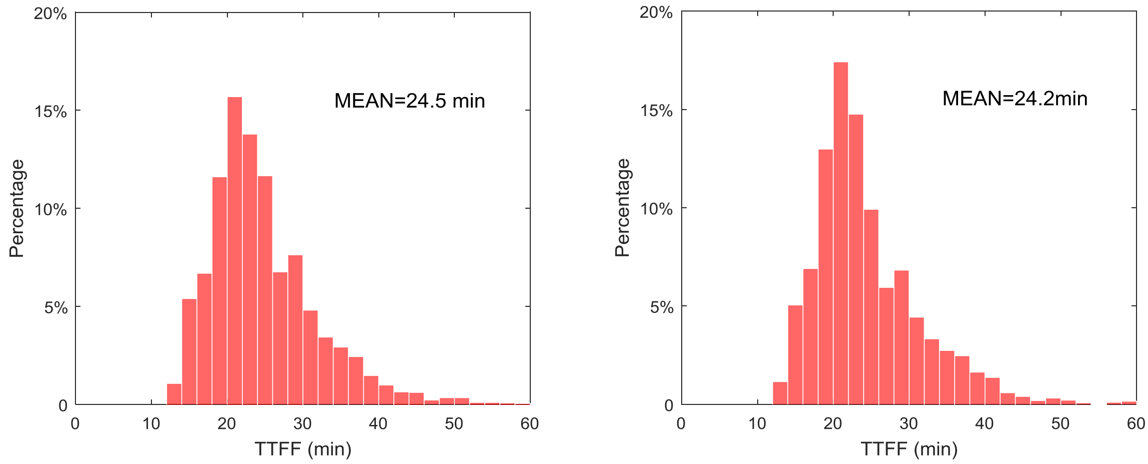

Figure 5. TTFF of FCB (*left*) and IRC (*right*) based PPP-AR

The average TTFF for FCB and IRC based PPP-AR is 24.5 and 24.2 min, respectively. Slightly better performance is also achieved with IRC based PPP-AR. We employ a strict ambiguity validation to decrease AR failure rate. As a result, it is obvious that the TTFF is much longer than the normal convergence time of IF-PPP to achieve the first ambiguity-fixed solution. If we decrease the threshold of success rate test and ratio test, i.e. to 0.99 and 2.0, TTFF can be further shortened but more ambiguities may be wrongly fixed. Therefore, there is a trade-off between the correct AR rate and the TTFF.

4.3 Impact of troposphere delay on PPP-AR

In order to evaluate the impact of troposphere delay on PPP-AR, four stations (FTDN, MGRV, PCTN and WFAL) from CORSnet-NSW in New South Wales, Australia were selected as a reference network and station VLWD was chosen as roving station. The distribution of the network stations is shown in Figure 6. The average inter-station distance is about 30km.

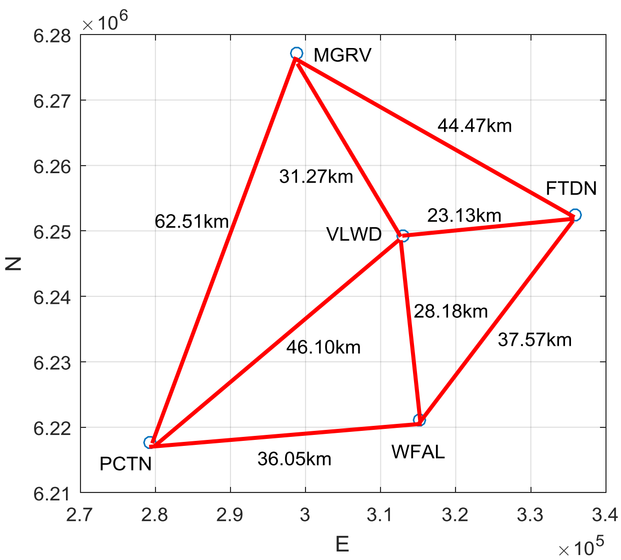

Figure 6. Distribution of the selected stations in CORSnet-NSW

Ambiguity-fixed and coordinate-fixed troposphere delays were firstly retrieved at the four reference stations, and then interpolated at VLWD according to the interpolation method discussed above. Compared with the ambiguity-fixed troposphere delay in VLWD, the troposphere delay residuals can be derived and shown in Figure 7.

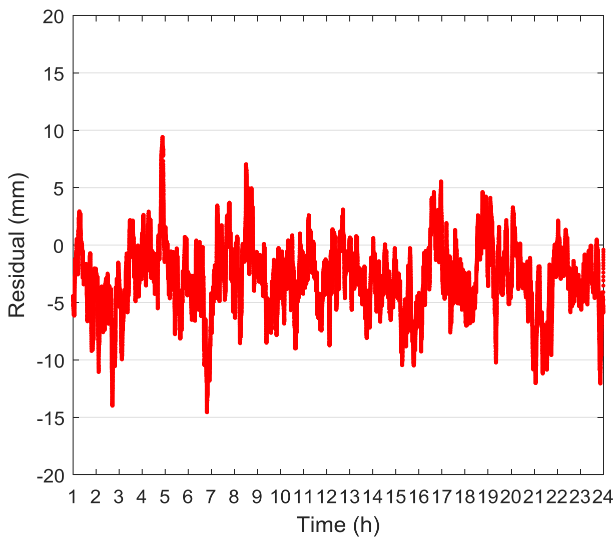

Figure 7. Troposphere delay residuals at station VLWD (1~24h)

It can be found that all the residuals are below 2cm. The RMS of residuals is about 5mm, which can be used to determine the stochastic model of troposphere delay pseudo observations to enhance the PPP-AR solutions. Figure 8 shows the PPP-AR solutions with and without troposphere delay constraint. It can be seen that the TTFF can be slightly shortened and vertical positioning accuracy can be significantly improved from decimetre to centimetre level with proper troposphere constraints.

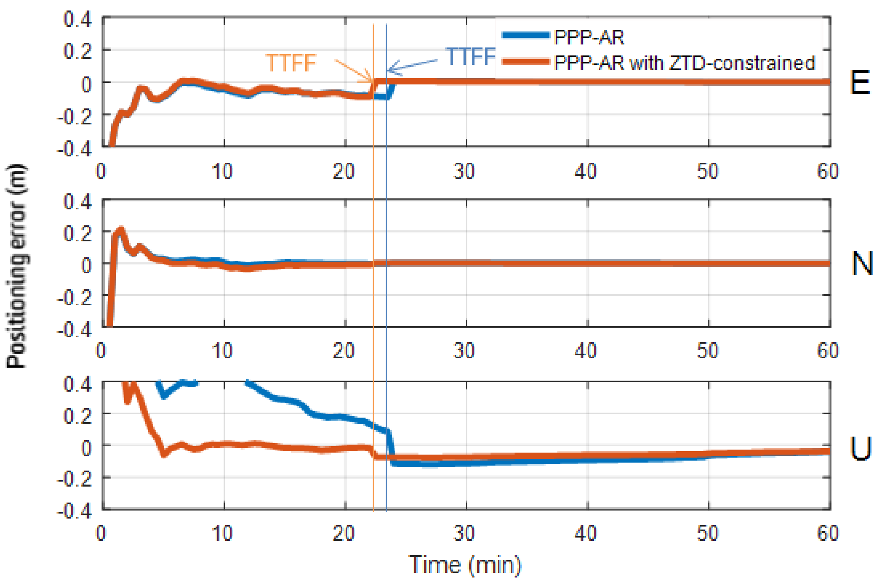

Figure 8. Comparison of PPP-AR solutions with and without troposphere delay constraint

In addition, we analysed the impact of troposphere delay on PPP-AR on a global scale. The same stations involved in FCB estimation were used. The troposphere products from IGS were employed as the constraints on the troposphere delay. The positioning results and TTFF for PPP-AR are summarized in Table 3. It is shown that the vertical accuracy and TTFF are both slightly improved.

	East	North	Up	3D	Mean TTFF
PPP-AR	**0.62cm**	**0.71cm**	**2.17cm**	**2.37cm**	**28.8min**
PPP-AR+TRO	**0.65cm**	**0.72cm**	**1.99cm**	**2.21cm**	**27.3min**

Table 3. Performance of PPP-AR with and without troposphere constraint

5. CONCLUDING REMARKS

Two types of PPP-AR methods, FCB and IRC based PPP-AR, are compared by theoretical and numerical analysis. They are proved to be theoretically equivalent but IRC based PPP-AR slightly outperforms FCB based PPP-AR due to the biased property of FCB estimation. Ambiguity fixing provides a considerable improvement in the positioning accuracy, especially in the east component, and vertical positioning accuracy can be improved with proper troposphere constraints.

However, even with the implementation of PPP-AR, the convergence time is still of the order of tens of minutes. In fact, the key issue of instantaneous PPP—AR is how to obtain the accurate ionosphere delay. Thus PPP-AR based on uncombined PPP model needs to be further investigated. Moreover, due to the biased property of FCB estimation, the quality control and reliability analysis of FCB estimation is crucial to FCB based PPP-AR. The famous ratio and success rate tests for integer ambiguity validation do not always work well for PPP.

The next step of our research will focus on quality control and reliability analysis of FCB based PPP-AR. Uncombined PPP model and multi-GNSS PPP will be studied as well. More rigorous integer ambiguity validation methods will be investigated to achieve reliable ambiguity-fixing PPP solutions.

ACKNOWLEDGEMENTS

The authors would like to thank the reviewers for their beneficial comments and suggestions. We also thank IGS and New South Wales Government for providing the data for this study.

REFERENCES

Bisnath S, Gao Y (2007) Current state of precise point positioning and future prospects and limitations. *Observing our changing planet*. *IAG Symposium* 133: 615-624

Collins P (2008) Isolating and estimating undifferenced GPS integer ambiguities. *Proceedings of ION NTM-2008*, San Diego, California, January, pp 720-732

Dach R, Brockmann E, Schaer S, Beutler G, Meindl M, Prange L, Bock H, Jäggi A, Ostini L (2009) GNSS processing at CODE: status report. *Journal of Geodesy* 83(3): 353-365

Ge M, Gendt G, Rothacher M, Shi C, Liu J (2008) Resolution of GPS carrier-phase ambiguities in precise point positioning (PPP) with daily observations. *Journal of Geodesy* 82(7): 389-399

Geng J, Meng X, Dodson A, Teferle F (2010) Integer ambiguity resolution in precise point positioning: method comparison. *Journal of Geodesy* 84(9): 569-581

Han S (1997) Carrier phase-based long-range GPS kinematic positioning. *Ph.D. Thesis*. School of Geomatic Engineering, The University of New South Wales, Sydney, Australia

Keshin MO, Le AQ, Marel H (2006) Single and dual-frequency precise point positioning: approaches and performance, *Proceedings of the 3rd ESA Workshop on Satellite Navigation User Equipment Technologies*, Noordwijk, pp 11-13

Kouba J, Héroux P (2001) Precise point positioning using IGS orbit and clock products, *GPS Solutions* 5(2): 12-28

Laurichesse D, Mercier F, Berthias J, Bijac J (2008) Real time zero-difference ambiguities blocking and absolute RTK. *Proceedings of ION NTM-2008*, San Diego, California, January, pp 747-755

Li X, Dick G, Lu C, Ge M, Nilsson T, Ning T, Wickert J, Schuh H (2015) Multi-GNSS meteorology: real-time retrieving of atmospheric water vapor from BeiDou, Galileo, GLONASS, and GPS observations. *IEEE Transactions on Geoscience and Remote Sensing* 53(12): 6385-6393

Li X, Ge M, Zhang Y, Wang R, Xu P, Wickert J, Schuh H (2013a) New approach for earthquake/tsunami monitoring using dense GPS networks. *Scientific Reports* 3: 2682

Li X, Ge M, Zhang H, Wickert J (2013b) A method for improving uncalibrated phase delay estimation and ambiguity-fixing in real-time precise point positioning. *Journal of Geodesy* 87(5):405-416

Loyer S, Perosanz F, Mercier F, Capdeville H, Marty J (2012) Zero-difference GPS ambiguity resolution at CNES-CLS IGS Analysis Center. *Journal of Geodesy* 86(11):991-1003

Melbourne W (1985) The case for ranging in GPS-based geodetic systems. *Proceedings of the first international symposium on precise positioning with the global positioning system*, Rockville, 15-19 April, pp 373-386

Schmid R, Rothacher M, Thaller D, Steigenberger P (2005) Absolute phase centre corrections of satellite and receiver antennas. *GPS Solutions* 9(4):283-293

Shi J, Gao Y (2013) A comparison of three PPP integer ambiguity resolution methods. *GPS Solutions* 18(4): 519-528

Shi J, Yuan X, Cai Y, Wang G (2016) GPS real-time precise point positioning for aerial triangulation. *GPS Solutions* 1-10. doi: 10.1007/s10291-016-0532-2

Teunissen PJG (1995) The least-squares ambiguity decorrelation adjustment method for fast GPS integer ambiguity estimation. *Journal of Geodesy* 70(1-2):65-82

Teunissen PJG, Khodabandeh A (2014). Review and principles of PPP-RTK methods, *Journal of Geodesy*, 89(3): 217-240

Wu J, Wu S, Hajj G, Bertiger W, Lichten S (1993) Effects of antenna orientation on GPS carrier phase. *Manuscripta Geodaetica* 18(2):91-98

Wubbena G (1985) Software developments for geodetic positioning with GPS using TI-4100 code and carrier measurements. *Proceedings of first international symposium on precise positioning with the global positioning system*, Rockville, 15-19 April, pp 403-412

Zumberge JF, Heflin MB, Jefferson DC, Watkins MM, Webb FH (1997) Precise point positioning for the efficient and robust analysis of GPS data from large networks, *Journal of Geophysical Research* 102 (B3): 5005-5017